Adaptive Periodic-Correlation Algorithm for Extended Scene Shack-Hartmann Wavefront Sensing

Erkin Sidick
Jet Propulsion Laboratory, California Institute of Technology, 4800 Oak Grove Drive, Pasadena, CA, USA 91109
Erkin.Sidick@jpl.nasa.gov

Abstract: We present an adaptive periodic-correlation algorithm for large dynamic range extended-scene Shack-Hartmann wavefront sensing. We show that it accurately measures very fine image shifts over many pixels under a variety of practical imaging conditions.
© 2007 Optical Society of America
OCIS codes: (100.5070) Phase retrieval; (110.6770) Telescopes

1. Introduction

The conventional method used in Shack-Hartmann wavefront sensor (SH-WFS) first produces a set of spot images from a point-source, then determines the positions of the centroids of these spot images, and finally retrieves the phase information from the estimates of the offsets between these centroid positions and a set of pre-determined reference positions. When used in a closed-loop wavefront sensing and control system of a telescope, it offers high dynamic range, albeit with a lower wavefront measurement resolution than, for example, the Modified Gerchberg-Saxton (MGS) WFS approach [1]. In some applications of space-based, airborne, and ground-based adaptive optical systems, an extended-scene Shack-Hartmann sensor (ES-SHS) provides some great benefits. Poyneer found that periodic correlation method works well in this application in terms of both performance with noise and computational simplicity [2]. In that approach, the sub-pixel shift between two sub-images is determined from the location of the cross-correlation peak of the two sub-images. Recently we proposed a new approach, the adaptive cross-correlation (ACC) algorithm, to estimate with high accuracy the shift as large as several pixels between two extended-scene images captured by an ES-SHS [3]. It determines the positions of all of the extended-scene sub-images or cells relative to a reference cell from the linear phase of the cross-correlation spectrum of the two cells. We tested the shift estimation accuracy of this approach with measured point-source and extended-scene images having several hundred cells. We compared its phase estimation accuracy with that of a conventional centroid-finding algorithm, and obtained good agreement between the two approaches.

Some applications in space telescope require an ES-SHS to have a large number of cells, say, for example, more than 1000 cells. We found that in such a case there can be a large-degree of non-uniformity among the cells contained in the same image captured by an SH camera (SHC), and the ACC algorithm does not provide the required accuracy, or sometimes fails completely. This is due to the fact that when two sub-images have a large-degree of dissimilarity, the linear phase of their cross-correlation spectrum can become very small even if there is a large amount of relative shift between the two cells. In order to solve this problem, we combined our "adaptive" procedure with the periodic correlation method and developed a new, alternative approach—the Adaptive Periodic-Correlation (APC) algorithm. In this paper we describe this new algorithm and present some simulation results.

2. Description of the Adaptive Periodic-Correlation Algorithm

The APC algorithm works in the same way as the ACC algorithm. The only difference is that, the ACC algorithm calculates the shift of a test cell relative to a reference cell from the linear phase component of the cross-correlation spectrum of the two cells. Whereas the APC algorithm calculates the same from the location of the cross-correlation peak in the image-domain. In our APC algorithm, the relative locations of the different SH extended-scene sub-images were determined in the following steps:

(1) Determine the center coordinates of all of the cells in Fig. 1(a), and store these x- and y-coordinate values in a [2xM] matrix. In our case, we used the centroid locations of a point-source spot image for this purpose.

(2) Choose an N_bxN_b pixel test cell, where N_b is preferentially a power of 2 for this algorithm and the subscript "b" means "big", within each sub-image with the x- and the y-coordinates determined in Step 1 as its center, as shown with a black-frame in Fig. 1(b). In this figure, the white-frame shows an 32x32 pixel cell. Also, choose one N_sxN_s small cell as a reference, where N_s<N_s and the subscript "s" means "small", preferably near the center of the extended-scene image. In the following, we use the position variables (x, y) to denote the position dependence of a cell in the image-domain, and use (u, v) to denote the position dependence of the Fourier-transform of a cell.

That is, the $r(x,y) \leftrightarrow \hat{r}(u,v)$ pair represents the reference cell in the original image and the Fourier domains, respectively. We represent the larger, N_bxN_b pixel test cells with the $S_i(x,y) \leftrightarrow \hat{S}_i(u,v)$ pair, and the smaller, N_sxN_s pixel test cells with the $s_i(x,y) \leftrightarrow \hat{s}_i(u,v)$ pair, respectively. As a standard procedure, we measure a dark image for every signal image and subtract it out from the signal image before processing the image data.

(3) Take the N_sxN_s pixel reference cell, $r(x,y)$, and calculate its Fourier-transform, $\hat{r}(u,v)$.

(4) Inside a for-loop with index *i*, select $S_i(x,y)$, and obtain the corresponding $\hat{S}_i(u,v)$ and $\hat{s}_i(u,v)$], respectively. Multiply $\hat{r}(u,v)$ and $\hat{s}_i(u,v)$ to obtain a cross-correlation function in Fourier-domain, $\hat{c}_i(u,v) = \hat{r}*(u,v)\hat{s}_i(u,v)$, where "*" denotes a complex-conjugate.

(5) Inside a while-loop with index *j*, take the inverse-FFT (Fast Fourier-Transform) of $\hat{c}_i(u,v)$ to obtain the cross-correlation function $c_i(x,y)$ in the spatial-domain.

(6) Fit a parabola to 3 pixels of $c_i(x,y)$ having $y = 0$ and $x = -1, 0, +1$, and determine the location of $c_i(x,y)$ peak in the horizontal or the x-direction, δx_{ij}. Do the same in the vertical or y-direction by fitting a parabola to 3 pixels of $c_i(x,y)$ having $x = 0$ and $y = -1, 0, +1$, and obtain δy_{ij}. In practice, each peak-location-finding is done analytically using 3 data points to determine 3 unknowns, *a*, *b*, and x_{max}[2]:

$$y = a(x - x_{\max})^2 + b \tag{1}$$

The [δx_{ij}, δy_{ij}] pair represent the incremental shifts in the x- and y-directions, respectively. Also accumulate these incremental shifts to obtain the total shifts [Δx_{ij}, Δy_{ij}] up to the current peak-finding iterations:

$$\Delta x_{ij} = \sum_j \delta x_{\mathrm{ij}}, \qquad \Delta y_{ij} = \sum_j \delta y_{\mathrm{ij}} \tag{2}$$

(7) Obtain a new $S_{ij}(x,y)$, a new version of $S_i(x,y)$ shifted to match with the $r(x,y)$, from the inverse-FFT of $\hat{S}_{ij}(u,v) = \hat{S}_i(u,v)\exp[-j2\pi(\Delta x_{ij}u + \Delta y_{ij}v)]$. Repeat the while-loop (Steps 5-6) until the radial incremental shift $\delta r_{ij} = \sqrt{\delta x_{ij}{}^2 + \delta y_{ij}{}^2}$ becomes less than a pre-determined tolerance value, such as 0.01 pixel, or until the total number of iterations, such as 15, is reached.

(8) Repeat the for-loop (Steps 4 through 7) for all test cells $S_i(x,y)$.

It should be pointed out that $\hat{r}(u,v)$ needs to be calculated only once for each SHC image, and $\hat{S}_i(u,v)$ needs to be calculated only once for each test cell. If the shift estimate for a particular test cell $s_i(x,y)$ is completed in 4 shift-finding iterations, then one needs to carry out inverse-FFT on $\hat{c}_{ij}(u,v)$ for 4 times (Steps 4-7), and calculate the inverse-FFT of $\hat{S}_{ij}(u,v) = \hat{S}_i(u,v)\exp[-j2\pi(\Delta x_{ij}u + \Delta y_{ij}v)]$ also 4 times.

3. Numerical examples and conclusion

We compared the current algorithm with the periodic-correlation method proposed by Poyneer in Ref. [2], by processing one set of ES-SHS image data measured on our testbed. We used the original 500x500 pixel image in Fig. 1(a) as the reference image, and generated a series of test images in the following way: (1) We created a 4x fine-sampled image by splitting each pixel of the original image into 4x4 pixels. (2) We introduced a known amount of x-shift into this new 4x-image by convolution. (3) We converted this shifted image back into a 500x500 pixel test image by binning it down by 4. We selected 4 pairs of cells from those two images, four reference cells from the reference image and four test cells from the test image such that the different test-reference cell pairs have slightly different centers on the corresponding sub-images. Then we estimated the shifts between those four pairs of test-reference cells using both the periodic correlation and the APC algorithms, as shown in Figs. 2(a) and 2(b), respectively. The radial shift estimate error is defined as $\sqrt{(\Delta x_{\mathrm{act}} - \Delta x_{\mathrm{est}})^2 + (\Delta y_{\mathrm{act}} - \Delta y_{\mathrm{est}})^2}$, where the subscripts "act" and "est" mean "actual" and "estimate", respectively. As we can see, the shift estimate accuracy is greatly improved in this new method. The average shift-finding iteration number ranged from 5.25 to 13 in this simulation. It must be pointed out that the only difference between the two algorithms is the number of shift-finding iterations: The original periodic correlation algorithm uses single iteration, whereas in the APC algorithm, that number is determined adaptively.

In conclusion, we have developed an adaptive cross-correlation algorithm for a Shack-Hartmann wavefront sensor. It is highly accurate when operating with both point-source images and extended scenes. We expect this algorithm to become widely useful in large dynamic range Shack-Hartmann wavefront sensing and control applications, including the SH systems used in ground and space based telescopes.

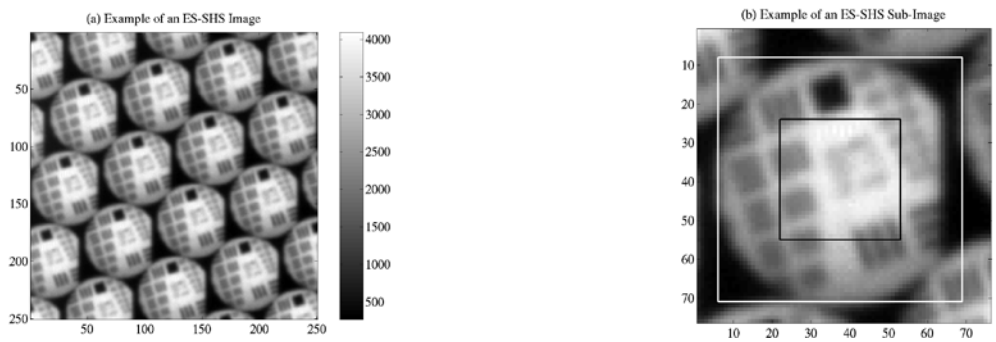

Figure 1. (a) An SH extended-scene sub-image array obtained with a bar target on our SH testbed. (b) One sub-image of the SH extended-scene. The white-colored box shows a 64x64 pixel (N_b=32) sub-aperture, and the black-colored box a 32x32 pixel (N_s=32) sub-aperture. These sub-apertures are referred to as big and small cells in this paper.

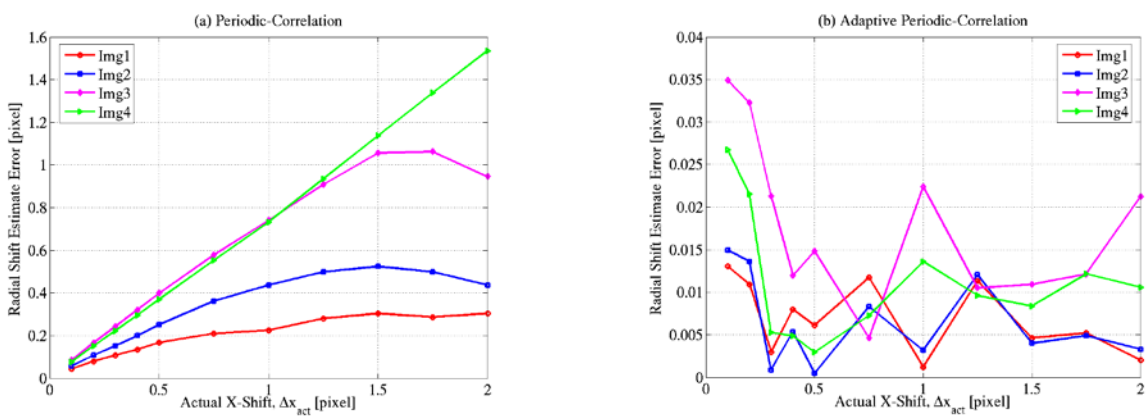

Figure 2. Numerical examples of shift estimation errors. (a) The results of the periodic-correlation algorithm, and (b) the corresponding results of the current Adaptive Periodic-Correlation (APC) algorithm.

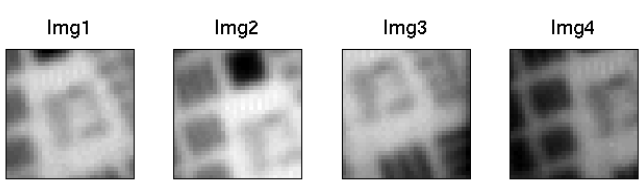

Figure 3. The four 32x32 pixel reference cells used in the current analysis. All four cells have the same color-stretch.

4. References

[1] Scott A. Basinger, David C. Redding, Andrew E. Lowman, Laura A. Burns, Karen Y. Liu, and David Cohen, "Performance of wavefront sensing and control algorithms on a segmented telescope testbed," Proc. SPIE Int. Soc. Eng. **4013**, 749 (2000).

[2] Lisa A. Poyneer, "Scene-based Shack-Hartmann wave-front sensing: analysis and simulation," Appl. Opt. **42**, 5807 (2003).

[3] E. Sidick, Joseph J. Green, Rhonda M. Morgan, Catherine M. Ohara, David C. Redding, "Adaptive cross-correlation algorithm for extended scene Shack-Hartmann wavefront sensing," Opt. Let. **33**, 213 (2008).